

PACS numbers: 68.55.-a, 72.25.Mk, 73.63.Bd, 73.90.+f, 75.47.De, 81.40.Ef

Phase State, Crystal Structure, Diffusion Processes and Magnetoresistance of Three-Layer Structures Based on $\text{Fe}_x\text{Co}_{1-x}$ ($x \cong 0.5$) and Cu

D. I. Saltykov, Yu. O. Shkurdoda, and I. Yu. Protsenko

Sumy State University,
2 Rymsky-Korsakov Str.,
UA-40007 Sumy, Ukraine

The comprehensive analysis of the phase state, crystal structure and magnetoresistive properties of three-layer films based on alloy $\text{Fe}_x\text{Co}_{1-x}$ ($x \cong 0.5$) and Cu is done. As shown, a phase state of as-deposited and annealed to 700 K films corresponds to the b.c.c. $\text{Fe}_x\text{Co}_{1-x}$ alloy (single-layer films) or b.c.c. $\text{Fe}_x\text{Co}_{1-x}$ + f.c.c. solid solution of Fe and Co atoms, which isomorphically replace each other in the Cu lattice (three-layer film). Annealing at the temperature of 700 K does not lead to complete mixing of the layers, their original order is maintained. For as-deposited three-layer film systems, the isotropic field dependences with maximum values of magnetoresistance (MR) (0.3%) for $d_F \cong 30$ nm (magnetic layers) and $d_N \cong 5$ nm (nonmagnetic layer) are fixed. The process of heat treatment of three-layer samples with $d_F \cong 20$ –30 nm, $d_N \cong 4$ –15 nm at a temperature of 550 K leads to 4–6 times increase of isotropic MR. Further annealing at a temperature of 700 K causes the appearance of anisotropic magnetoresistance.

Key words: three-layer film, phase composition, spin-dependent electron scattering, magnetoresistance.

Проведено комплексне дослідження структурно-фазового стану та магніторезистивних властивостей тришарових плівок на основі сплаву $\text{Fe}_x\text{Co}_{1-x}$ ($x \cong 0.5$) та Cu. Показано, що як у свіжосконденсованих, так і у відпалених до 700 К плівках фазовий склад відповідає сплаву ОЦК- $\text{Fe}_x\text{Co}_{1-x}$ (одно-

Corresponding author: Ivan Yukhymovych Protsenko
E-mail: i.protsenko@aph.sumdu.edu.ua

Citation: D. I. Saltykov, Yu. O. Shkurdoda, and I. Yu. Protsenko, Phase State, Crystal Structure, Diffusion Processes and Magnetoresistance of Three-Layer Structures Based on $\text{Fe}_x\text{Co}_{1-x}$ ($x \cong 0.5$) and Cu, *Metallofiz. Noveishie Tekhnol.*, **41**, No. 5: 595–605 (2019), DOI: [10.15407/mfint.41.05.0595](https://doi.org/10.15407/mfint.41.05.0595).

шарові плівки) або ОЦК- $\text{Fe}_x\text{Co}_{1-x}$ + ГЦК-твердий розчин атомів Fe і Co, які ізоморфно заміщують один одного в решітці Cu (тришарова плівка). Відпалювання до температури 700 К не призводить до повного перемішування шарів, їх вихідний порядок зберігається. Для тришарових свіжосконденсованих плівкових систем фіксуються ізотропні польові залежності з максимальним значенням магнітоопору (МО) (0,3%) для плівок з магнітними і немагнітним шарами з $d_F \cong 30$ нм та $d_N \cong 5$ нм відповідно. Термообробка тришарових зразків з $d_F \cong 20-30$ нм, $d_N \cong 4-15$ нм за температури 550 К призводить до збільшення ізотропного МО в 4-6 разів. Подальше відпалювання за температури 700 К спричиняє появу анізотропного магнітоопору.

Ключові слова: тришарові плівки, фазовий склад, спин-залежне розсіювання електронів, магнітоопір.

Проведено комплексное исследование структурно-фазового состояния и магниторезистивных свойств трёхслойных плёнок на основе сплава $\text{Fe}_x\text{Co}_{1-x}$ ($x \cong 0,5$) и Cu. Показано, что как в свежесконденсированных, так и в отожжённых до 700 К плёнках фазовый состав соответствует сплаву ОЦК- $\text{Fe}_x\text{Co}_{1-x}$ (однослойные плёнки) или ОЦК- $\text{Fe}_x\text{Co}_{1-x}$ + ГЦК-твёрдый раствор атомов Fe и Co, которые изоморфно замещают друг друга в решётке Cu (трёхслойная плёнка). Отжиг до температуры 700 К не приводит к полному перемешиванию слоёв, их исходный порядок сохраняется. Для трёхслойных свежесконденсированных плёночных систем фиксируются изотропные полевые зависимости с максимальным значением магнитосопротивления (МС) (0,3%) для плёнок с магнитными и немагнитным слоями с $d_F \cong 30$ нм и $d_N \cong 5$ нм соответственно. Термообработка трёхслойных образцов с $d_F \cong 20-30$ нм, $d_N \cong 4-15$ нм при температуре 550 К приводит к увеличению изотропного МС в 4-6 раз. Дальнейший отжиг при температуре 700 К вызывает появление анизотропного магнитосопротивления.

Ключевые слова: трёхслойные плёнки, фазовый состав, спин-зависимое рассеяние электронов, магнитосопротивление.

(Received October 3, 2018)

1. INTRODUCTION

During the last decades, systematic studies of thin films of 3d-metals and structures on their basis have been carried out. Features of their structural, electrophysical and magnetoresistive properties have been revealed. The research results have contributed to their use for the manufacture of various types of apparatus and devices of modern electronics [1-3]. The possibility of creating materials with predetermined properties expanded with the use of magnetic film alloys. Particularly relevant was the study of these alloys after the discovery of the phenomenon of a giant magnetoresistance (GMR) in multilayer systems, which consist of ferromagnetic layers separated by a nonmagnetic

spacer. Such systems are now the objects of experimental and theoretical studies. It should be noted that in a majority of works, where such structures were investigated, Permalloy used as magnetic layers ($\text{Fe}_{20}\text{Ni}_{80}$ and $\text{Fe}_{50}\text{Ni}_{50}$) [3, 4]. Much less attention is paid to the study of the physical properties of multilayer structures based on $\text{Fe}_x\text{Co}_{1-x}$ alloy in a wide range of concentrations obtained under the same conditions. Analysis of these works [5, 6] shows that the physical properties of $\text{Fe}_x\text{Co}_{1-x}$ alloys and multilayer films based on them significantly depend on the concentration of components, crystal structure and phase composition. A number of studies have shown that superlattices $\text{Co}_{0.9}\text{Fe}_{0.1}/\text{Cu}$ also have a relatively high magnitude of the GMR effect and low saturation fields that generate considerable interest for application uses [7, 8].

The aim of this work is to study the phase state and crystal structure, diffusion processes and magnetoresistive properties for as-deposited and annealed $\text{Fe}_x\text{Co}_{1-x}$ ($x \cong 0.5$) film alloys and three-layer systems on their basis in a wide range of thicknesses as the magnetic (d_F) layers and Cu nonmagnetic (d_N) layer. Note that it is a logical continuation of our previous study [9] of the crystal structure and magnetoresistive properties of similar $\text{Fe}_x\text{Co}_{1-x}/\text{Cu}/\text{Fe}_x\text{Co}_{1-x}/\text{S}$ three-layer structures.

2. EXPERIMENTAL

Single-layer films and three-layer film systems with a thickness of layers (1–50) nm were obtained in a vacuum chamber at the pressure of the gases of the residual atmosphere of 10^{-4} Pa. Layer-by-layer films condensation was carried out by evaporation of metals from independent sources (Cu—from a tungsten tape, $\text{Fe}_x\text{Co}_{1-x}$ —by an electron beam gun). The starting material for the production of $\text{Fe}_x\text{Co}_{1-x}$ layers was massive alloys of the corresponding composition ($x \cong 0.5$).

The film condensation was carried out on the substrate at room temperature with a speed of $\omega = 0.5\text{--}1$ nm/s, depending on the operating conditions of the evaporators. For study magnetoresistive properties, glass plates with pre-deposited contact pads were used as the substrate. The design of the lining holder allowed receiving two film samples with a different thickness of the nonmagnetic layer and with similar thicknesses of the ferromagnetic ones in one technological cycle. For measuring their electrical resistance, the geometric dimensions of the films were set by windows in the nichrome foil mechanical masks, which made with high accuracy.

The thickness of the films was determined using a Linnik microinterferometer with a laser light source and a computer system for recording interference pattern, which allowed to increase the accuracy of measurements, especially in the case when thickness $d < 50$ nm (up to

20%).

The concentration of the components in the magnetic layers was calculated based on the mass of metals loaded into the evaporator. The results of the study of the chemical composition of the initial alloy $\text{Fe}_x\text{Co}_{1-x}$ and deposited films investigated by the method of X-ray microanalysis show that they coincide with the error of measurement.

Measurement of longitudinal (\parallel) and transverse (\perp) magnetoresistance (MR) (magnetic field in the film plane) and thermomagnetic investigations of films was held in a special device under ultrahigh oil-free vacuum (10^{-6} – 10^{-7}) Pa in the magnetic field with induction to $B = 0.2$ T. The films were annealed according to the scheme ‘heating–exposure at temperatures of 400, 550 and 700 K for 15 minutes–cooling’.

The magnitude of the longitudinal and transverse magnetoresistance of the film samples was calculated as $(R(B) - R(B_c))/R(B_c)$, where $R(B)$ is the sample resistance in the magnetic field with induction B ; $R(B_c)$ is the resistance of the sample in the field of the coercive force B_c .

A qualitative analysis of the elemental composition of films was carried out using a secondary-ion mass spectrometry (SIMS) using a mass spectrometer MS-7201M. The obtained data in the layer etching of the film with argon ions were used to construct concentration profiles along the sample depth. The percentage composition of the film was determined by X-ray microanalysis with energy dispersive spectrometer (EDS).

3. RESULTS AND DISCUSSION

For preparing of thin films of $\text{Fe}_x\text{Co}_{1-x}$ ($x \cong 0.5$) ferromagnetic alloy, which was a part of the three-layer structures, we used the method of evaporation of the finite batches. To check that composition of the prepared thin film alloy coincides to the composition of the batches, the X-ray microanalysis using Scanning electron microscope with an energy dispersive detector to perform the X-ray spectrometry (EDX) was carried out.

Figure 1 shows the results of the investigation of $\text{Fe}_x\text{Co}_{1-x}/\text{Cu}/\text{Fe}_x\text{Co}_{1-x}$ film composition. The characteristic X-ray line at the left side of the spectrum from $\text{Fe}_x\text{Co}_{1-x}$ film alloys and three-layer films based on them corresponds to the substrate material. The error of determining the elemental composition of film samples does not exceed 2%.

Crystal structure, phase and elemental composition of the magnetic layers that a part of total film system is defining features of its magnetic and magnetoresistive properties. Therefore, the phase state and crystal structures investigations for as-deposited and annealed up to

700 K $\text{Fe}_x\text{Co}_{1-x}$ single-layer film alloy (Fig. 2, *a-d*) were carried out. According to the data of electron microscopic and electronographic investigations for both as-deposited and annealed at 700 K samples with thickness $d_F = 10-80$ nm, their phase composition corresponds to b.c.c. $\text{Fe}_x\text{Co}_{1-x}$ with lattice parameter $a = 0.292-0.293$ nm. (Fig. 2, *b, d*, Table 1). All films are polycrystalline with grain size about 5 nm in as-deposited state (Fig. 2, *a*) and 30–50 nm after heat treatment at a temperature of 700 K (Fig. 2, *b*). Similar results were obtained in [6, 9].

In the case of three-layer $\text{Fe}_x\text{Co}_{1-x}/\text{Cu}/\text{Fe}_x\text{Co}_{1-x}/\text{S}$ films with $d_F = 20-40$ nm, $d_N = 5-20$ nm, the phase composition corresponds to the eutectic of the b.c.c. $\text{Fe}_x\text{Co}_{1-x}$ + f.c.c. of the Fe and Co atoms in the Cu lattice with a possible isomorphous substitution of Fe and Co atoms regardless of the heat treatment conditions (Fig. 2, *f, h*, Table. 2). This is evidenced by the values of lattice parameters (Table 1 and 2). Note that the lattice of solid solution (s.s.) Cu (Fe or Co) has tetragonal distortion (Fig. 2, *h*); therefore it can be interpreted as the f.c.t. lattice.

SIMS method confirmed the effectiveness of methods that used to obtain film alloys. The intensity ratio of mass spectrometry isotope peaks ^{56}Fe and ^{59}Co $\gamma = J(^{59}\text{Co})/J(^{56}\text{Fe})$ was used for estimation the content of the components in the alloy. Comparison of γ for the same film alloy depending on the time of etching of the sample by the primary ion beam of Ar^+ shows that within the error of the measurement value γ does not change. Hence, the resulting films of the $\text{Fe}_x\text{Co}_{1-x}$ alloy are homogeneous in thickness.

The results demonstrate that the individuality of the individual layers for two- and three-layer samples after deposition remained regardless of the layer thickness. The negligible blurring of interfaces is a result of the atom diffusion during condensation and ion-stimulated diffusion (Fig. 3, *a, c, f*). As a result, the systems of the eutectic type formed. The concentration profiles presented at Fig. 3 for the Cu, Fe, and Co atoms should not interpret as a complete atom mixing. The point we want to make that part of FeCo molecules dissociate during

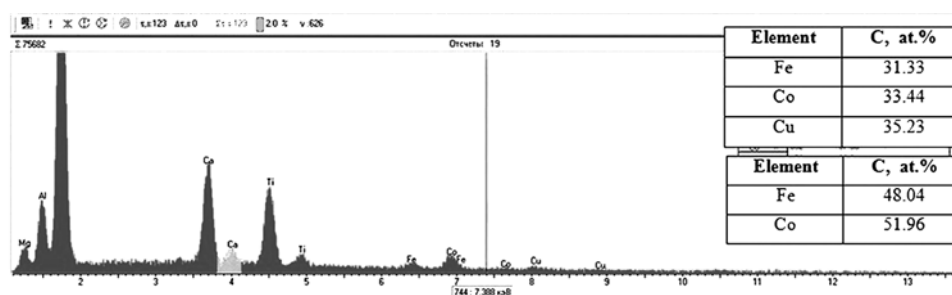


Fig. 1. Characteristic X-ray spectrum for $\text{Fe}_x\text{Co}_{1-x}/\text{Cu}/\text{Fe}_x\text{Co}_{1-x}$ three-layer film with $d_F = 20$ nm and $d_N = 20$ nm.

evaporation and, especially, during the interaction of the primary ion beam with the sample. Just these atoms take part in mutual diffusion, though the identity of top and bottom retained in general.

Heat treatment of the samples at 700 K does not lead to complete mixing of layers. Insignificant penetration of the elements of the second layer on the surface of the sample is probably caused by grain boundary thermodiffusion.

It should be noted that in the case of step-by-step annealing (through intermediate temperatures of 400 and 550 K), the mutual penetration of the atoms of Co, Fe, and Cu in the adjacent layers is more significant than in the case of heating directly up to 700 K. This leads to disruption of structural continuity of the copper layer. As a result, film systems with $d_F = 20\text{--}40$ nm and $d_N = 10\text{--}20$ nm characterized by the isotropic magnetoresistance after heat treatment directly up to 700 K, whereas the process step-by-step annealing leads to the anisotropic

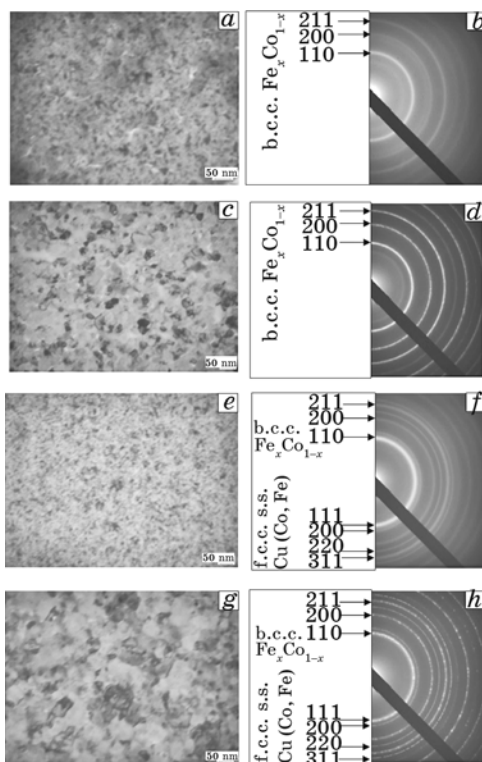


Fig. 2. TEM and TEM diffractions images of the $\text{Fe}_x\text{Co}_{1-x}$ ($x \cong 0.5$) single-layer films with thickness 50 nm (*a–d*) and $\text{Fe}_x\text{Co}_{1-x}/\text{Cu}/\text{Fe}_x\text{Co}_{1-x}$ film structures with $d_F = 30$ nm, $d_N = 7$ nm (*e–h*) at the as-deposited (*a, b, e, f*) and annealed at 700 K (*c, d, g, h*) states.

TABLE 1. Analysis of the TEM diffraction images for the as-deposited and annealed in a vacuum ($p \sim 10^{-6}$ Pa) at 700 K $\text{Fe}_x\text{Co}_{1-x}$ sample with thickness 50 nm (v.s.—very strong, a.—average, w.—weak).

As-deposited					Annealed at 700 K					
I , r.u.	d , Å	hkl	Phase	a , Å	I , r.u.	d , Å	hkl	Phase	a , Å	a_0 , Å
v.s.	2.060	110	b.c.c. $\text{Fe}_x\text{Co}_{1-x}$	2.913	v.s.	2.019	110	b.c.c. $\text{Fe}_x\text{Co}_{1-x}$	2.854	2.861 (α -Fe)
w.	1.456	200	b.c.c. $\text{Fe}_x\text{Co}_{1-x}$	2.912	a.	1.427	200	b.c.c. $\text{Fe}_x\text{Co}_{1-x}$	2.854	
a.	1.187	211	b.c.c. $\text{Fe}_x\text{Co}_{1-x}$	2.909	a.	1.163	211	b.c.c. $\text{Fe}_x\text{Co}_{1-x}$	2.849	

TABLE 2. Analysis of the TEM diffraction images for the as-deposited and annealed in a vacuum ($p \sim 10^{-6}$ Pa) at 700 K $\text{Fe}_x\text{Co}_{1-x}/\text{Cu}/\text{Fe}_x\text{Co}_{1-x}$ sample ($x \cong 0.5$, $d_F = 30$ nm, $d_N = 10$ nm).

As-deposited					Annealed at 700 K					
I , r.u.	d , Å	hkl	Phase	a , Å	I , r.u.	d , Å	hkl	Phase	a , Å	a_0 , Å
v.s.	2.084	110	b.c.c. $\text{Fe}_x\text{Co}_{1-x}$ f.c.c. s.s. Cu	2.946	v.s.	2.058	110	b.c.c. $\text{Fe}_x\text{Co}_{1-x}$ f.c.c. s.s. Cu	2.910	2.861 (α -Fe)
		111	(Fe, Co)	3.609			111	(Fe, Co)	3.564	
w.	1.860	200	f.c.c. s.s. Cu (Fe, Co)	3.720	a.	1.842	200	f.c.c. s.s. Cu (Fe, Co)	3.683	
a.	1.455	200	b.c.c. $\text{Fe}_x\text{Co}_{1-x}$	2.911	a.	1.457	200	b.c.c. $\text{Fe}_x\text{Co}_{1-x}$	2.914	
a.	1.307	220	f.c.c. s.s. Cu (Fe, Co)	3.671	a.	1.307	220	f.c.c. s.s. Cu (Fe, Co)	3.697	
a.	1.191	211	b.c.c. $\text{Fe}_x\text{Co}_{1-x}$	2.919	a.	1.195	211	b.c.c. $\text{Fe}_x\text{Co}_{1-x}$	2.927	

magnetoresistance appearance.

Consider more detail the results of the magnetoresistance investigations for as-deposited and annealed at 400 and 550 K three-layer films within the range of thicknesses $d_N = 3\text{--}15$ nm and $d_F = 20\text{--}40$ nm. All field dependencies characterized by isotropy magnetoresistance that is a sign of giant magnetoresistance (Fig. 4, *a*). Note that a negative value of the magnetoresistance in Fig. 4 is a result of the decrease of the electrical resistance $R(B)$ of the sample at its introduced into a magnetic field B . In addition, a hysteresis of the magnetoresistance effect is observed regardless of the thickness of both magnetic and nonmagnetic layers.

In these structures, a relatively weak magnetic field transits the system from antiferromagnetic to ferromagnetic ordering, which leads

to decrease the resistance of the sample and as a result of GMR effect realizing [10]. It should be noted that the effect of giant magnetoresistance does not depend on the relative orientation of the magnetic field and current, and depends on the relative orientation of the magnetization in the adjacent ferromagnetic layers [11]. In the case of antiparallel magnetization of adjacent magnetic layers, the electrical resistance of the sample is greater than in the case of their parallel magnetization.

The origin of giant magnetoresistance in multilayer films is the spin-dependent scattering of conducting electrons at the interfaces be-

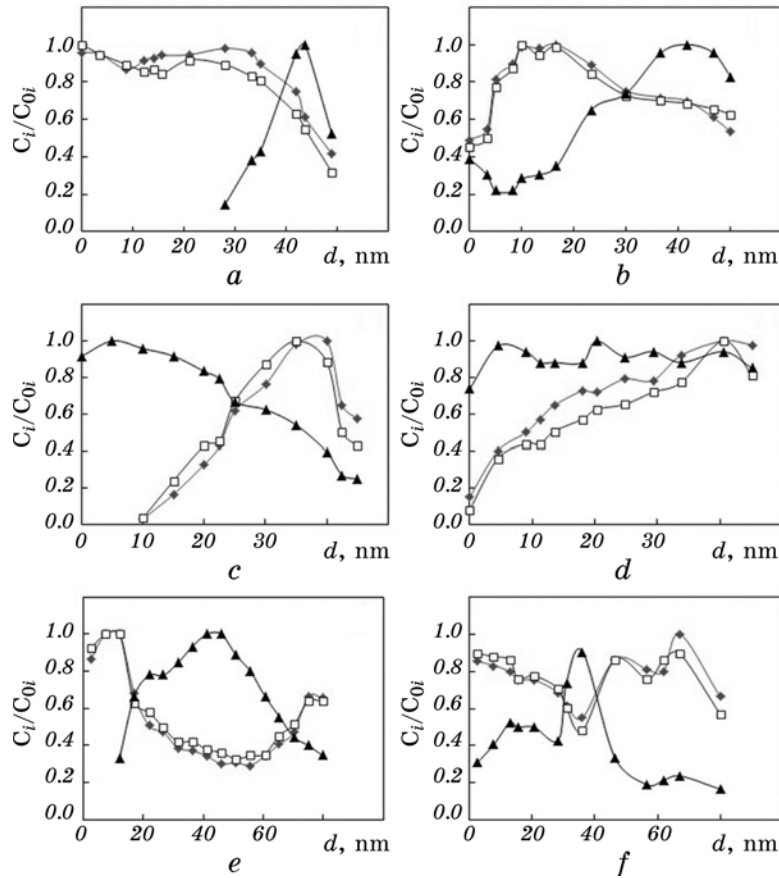


Fig. 3. Concentration profiles for $\text{Fe}_x\text{Co}_{1-x}(30\text{ nm})/\text{Cu}(20\text{ nm})/\text{S}$ (*a*, *b*), $\text{Cu}(20\text{ nm})/\text{Fe}_x\text{Co}_{1-x}(25\text{ nm})/\text{S}$ (*c*, *d*) and $\text{Fe}_x\text{Co}_{1-x}(30\text{ nm})/\text{Cu}(20\text{ nm})/\text{Fe}_x\text{Co}_{1-x}(30\text{ nm})/\text{S}$ (*f*, *g*) systems (\blacklozenge —Fe, \blacktriangle —Cu, \square —Co) in as-deposited (*a*, *c*, *f*) and annealed states at a temperature of 700 K (*b*, *d*, *g*); C_i is the concentration of the i -th element at the thickness change, C_{0i} is the maximum of concentration of the i -th element.

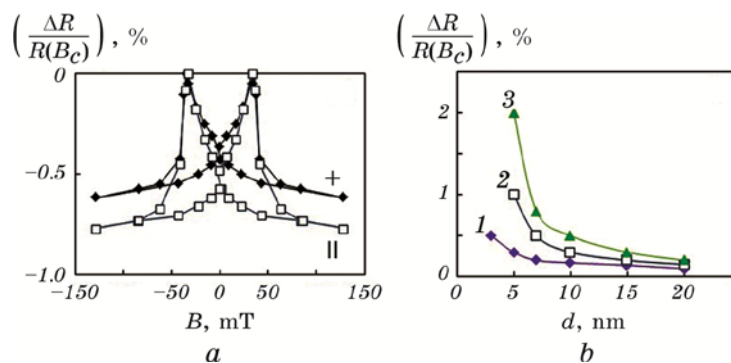


Fig. 4. Field dependences of longitudinal (||) and transverse (+) magnetoresistance (a) and size dependencies (b) of the isotropic magnetoresistance for as-deposited (1) and annealed at 400 (2) and 550 K (3) $\text{Fe}_x\text{Co}_{1-x}/\text{Cu}/\text{Fe}_x\text{Co}_{1-x}/\text{S}$ films: $d_F = 20$ nm and $d_N = 5$ nm (a), $d_F = 20$ nm (b).

tween magnetic and nonmagnetic layers and in the volume of metal layers [12].

The dependence of isotropic magnetoresistance on the thickness of the copper layer is shown in Fig. 4, b. These data indicate that the maximum value of GMR is observed at the effective thickness of the copper layer $d_N = 4\text{--}10$ nm, depending on the conditions of heat treatment. For as-deposited films, minimum effective thicknesses of the nonmagnetic layer, in which the isotropic field dependence is realized, is $d_N = 3\text{--}4$ nm. The increase of annealing temperature leads to increase of the minimum value of copper layer thickness to 10 nm, in which the isotropic field dependences of the magnetoresistance is realized, due to the increase of the interfaces width. The anisotropic character of the magnetoresistance for small effective copper thicknesses is associated with the presence of a relatively large number of microholes in it. The highest value of GMR at room temperature (2%) was observed for films with $d_N \cong 7$ nm after heat-treating at 550 K [13]. A further increase of the nonmagnetic interlayer thickness is also reduced $(\Delta R/R)_{\text{max}}$ through the scattering of electrons in the volume. In contrast to the size dependences presented in [6, 14, 15], in our case, no oscillations were observed as a result of relatively large effective interlayer thicknesses and, as a consequence, a significant weakening of the exchange interaction between the magnetic layers.

4. SUMMARY

According to the data of electron microscopic and electronographic investigations for both as-deposited and annealed at 700 K samples with thickness $d_F = 10\text{--}80$ nm, their phase composition corresponds to b.c.c.

$\text{Fe}_x\text{Co}_{1-x}$ with lattice parameter $a = 0.292\text{--}0.293$ nm. In the case of $\text{Fe}_x\text{Co}_{1-x}/\text{Cu}/\text{Fe}_x\text{Co}_{1-x}$ three-layer films with $d_F = 20\text{--}40$ nm and $d_N = 5\text{--}20$ nm, the phase composition corresponds to a disordered b.c.c $\text{Fe}_x\text{Co}_{1-x} + \text{f.c.c. s.s.}$ of the Fe and Co atoms in the Cu lattice, regardless of the heat treatment conditions.

The method of secondary ion mass spectrometry showed that $\text{Fe}_x\text{Co}_{1-x}$ ($x \cong 0.5$) alloys are homogeneous in thickness. In the $\text{Fe}_x\text{Co}_{1-x}/\text{Cu}/\text{Fe}_x\text{Co}_{1-x}$ three-layer films the identity of layers remained regardless of their thickness. The thermo- and ion-stimulated diffusion leads to mutual diffusion of Fe and Co atoms, which appear as a result of the dislocation of the FeCo molecules and Cu. The heat treatment at 700 K does not lead to the complete mixing of the layer. Their original order remains unchanged.

For as-deposited $\text{Fe}_x\text{Co}_{1-x}/\text{Cu}/\text{Fe}_x\text{Co}_{1-x}$ three-layer film systems with $x \cong 0.5\%$ wt. and $d_N = 3\text{--}10$ nm, isotropic field dependences are observed as a result of the realization of spin-dependent electron scattering. The maximum value of isotropic MR (0.3%) at room temperature is observed for films with $d_F \cong 30$ nm and $d_N \cong 5$ nm. The heat treatment of three-layer samples with $d_F = 20\text{--}30$ nm, $d_N = 4\text{--}15$ nm at 550 K leads to increase of isotropic magnetoresistance in 4–6 times. At the same time, the annealing at 700 K leads to the appearance of anisotropic magnetoresistance.

This work was funded by the State Program of the Ministry of Education and Science of Ukraine No. 0118U003580 (2018–2020).

REFERENCES

1. A. M. Pogorily, S. M. Ryabchenko, and A. I. Tovstolytkin, *Ukrayins'kyy Fizychnyy Zhurnal Rev.*, **6**, No. 1: 37 (2010).
2. C. D. Damsgaard, B. T. Dalslet, S. C. Freitas, P. P. Freitas, and M. F. Hansen, *Sens. Actuators A*, **156**, No. 1: 103 (2009).
3. O. I. Tovstolytkin, M. O. Borovyv, V. V. Kurylyuk, and Yu. A. Kunyts'kyy, *Fizychni Osnovy Spintroniky* [Physical Foundations of Spintronics] (Vinnytsia: Nilan-LTD: 2014) (in Ukrainian).
4. Yu. O. Shkurdoda, I. M. Pazukha, and A. M. Chornous, *Intermetallics*, **93**: 1 (2018).
5. Turgut Sahin, Hakan Kockar, and Mursel Alper, *J. Magn. Magn. Mater.*, **373**: 128 (2015).
6. E. M. Kakuno, D. H. Mosca, I. Mazzaro, N. Mattoso, W. H. Schreiner, M. A. B. Gomes, and M. P. Cantro, *J. Electrochem. Soc.*, **144**, No. 9: 3222 (1997).
7. Ikuo Ohnuma, Hirotohi Enoki, Osamu Ikeda, Ryosuke Kainuma, Hiroshi Ohtani, Bo Sundman, and Kiyohito Ishida, *Acta Mater.*, **50**, No. 2: 379 (2002).
8. E. Y. Tsymbal and D. G. Pettifor, *Solid State Phys.*, **56**: 113 (2001).
9. D. I. Saltykov, Yu. O. Shkurdoda, and I. Yu. Protsenko, *J. Nano-Electron. Phys.*, **10**, No. 4: 04031 (2018).

10. S. K. J. Lenczowski, M. A. M. Gijs, J. B. Giesbers, R. J. M. van de Veerdonk, and W. J. M. de Jonge, *Phys. Rev. B*, **50**, No. 14: 9982 (1994).
11. M. N. Baibich, J. M. Broto, A. Fert, F. Nguyen Van Dau, F. Petroff, P. Etienne, G. Creuzet, A. Friederich, and J. Chazelas, *Phys. Rev. Lett.*, **61**, No. 21: 2472 (1988).
12. S. S. P. Parkin, *Annu. Rev. Mater. Sci.*, **25**: 357 (1995).
13. Ia. M. Lytvynenko, I. M. Pazukha, and V. V. Bibyk, *J. Nano-Electron. Phys.*, **6**, No. 2: 02014 (2014).
14. E. M. Kakuno, R. C. da Silva, N. Mattoso, W. H. Schreiner, D. H. Mosca, and S. R. Teixeira, *J. Phys. D: Appl. Phys.*, **32**, No. 11: 1209 (1999).
15. Y. Jyoko, S. Kashiwabara, Y. Hayashi, and W. Schwarzacher, *J. Magn. Magn. Mater.*, **198–199**: 239 (1999).